Water Level Detection in Adverse Weather Conditions Using Security Cameras

Aref Shiran*, Jian Li*, Yonghe Liu*, Michelle Hummel†, Oswald Jenewein§, Karabi Bezboruah‡
*Department of Computer Science, The University of Texas at Arlington, USA
†Department of Civil Engineering, University of Texas at Arlington, USA
‡Department of Public Affairs and Planning, University of Texas at Arlington, USA
§ School of Architecture, University of Texas at Arlington, USA
Email:aref.shiran@uta.edu,jian.li3@mavs.uta.edu,yonghe@cse.uta.edu,
michelle.hummel@uta.edu, oswald.jenewein@uta.edu, bezborua@uta.edu

***Abstract*—Various techniques in computer vision have been proposed for water level detection. However, existing methods face challenges during adverse conditions including snow, fog, rain, and nighttime. In this paper, we introduce a novel approach that analyzes images for water level detection by incorporating a deblurring process to increase image clarity. By employing real-time object detection technique YOLOv5, we show that the proposed approach can achieve significantly improved precision, during both daytime and nighttime under under challenging weather circumstances.**

***Index Terms*—Improved YOLOv5s, Target detection, Intelligent agriculture, Water level**

I. Introduction

Monitoring water levels is essential for managing water resources and ensuring environmental safety. Water level data is often crucial for accurately predicting flood control in areas near rivers, seas, and lakes [1], [2]. Continuous measuring of water levels is increasingly essential for preventing urban flooding and minimizing associated damages and resulting recovery costs [3]–[5]. In coastal regions, water level changes can also be introduced by movements of large ships such as supertankers, posing unique environmental risks due to potential flooding, increased erosion, and damage to marine ecosystems and infrastructures [6]. Awareness of these changes is critical in understanding and managing the impact of ship movements.

Water level measurement methods can generally be categorized into two traditional approaches: contact-based and non-contact-based. Contact-based approaches are based on various sensors placed directly in the water, such as submersible pressure sensors, to measure water levels. While these sensors are often convenient, with long proven records, they present potential challenges, including high costs, installation difficulties, and maintenance requirements [9]. Further, they are often subject to fouling accumulation, leading to inaccurate readings [11]. In contrast, non-contact sensors like radar or ultrasonic sensors offer several advantages. They require much less maintenance and consume significantly less power [10]. However, installation limitations exist, as mounting them on bridges or poles can introduce measurement errors due to vibrations generated by these structures [10]. Recently, numerous computer vision techniques have been developed as non-contact approaches, enhancing the precision of water level detection methods [11], [15]. However, these methods need help under challenging weather conditions, which can compromise the quality of images or videos of the measuring gauges. Such degradation, in turn, can lead to inaccuracies in determining the water level.

To address the shortcomings of computer vision approaches in adverse weather conditions, we have developed a cost-effective method for detecting water levels that perform effectively across various weather conditions while leveraging existing commonly available, off-the-shelf security cameras. After gathering video data from security cameras, we first assess the image quality using a threshold based method. For images with quality falling below the given threshold, we then enhance the image quality by perform deblurring. Subsequently, images that meet the quality standards will be fed into our waterline detection scheme based on the YOLOv5 framework [12] [13], known for its speed and precision.

The rest of this paper is structured as follows. Section II presents the literature review of existing methods for staff gauge detection and water level monitoring. Section III details the proposed approach. Section IV presents the performance evaluation, followed by the conclusion and future work in Section V.

II. Related Work

Low image or video quality poses significant challenges in methods designed for detecting water levels. To address this problem, numerous computer vision techniques have been developed and refined. [7], [11], [14]. The authors in [14] tackle image noises by applying a Gaussian filter to smooth gray-scale images and remove noises. To further enhance accuracy, they also introduce photogrammetric methods to track camera movements, ensuring precise water level measurements in the object space. However, the authors note that identifying the water line in images of water gauges is challenging at night due to low light. Additionally, the proposed water line detection algorithm requires the water to be relatively still to work effectively.

In [7], the authors employ the Otsu technique for straightforward image segmentation, separating the foreground and

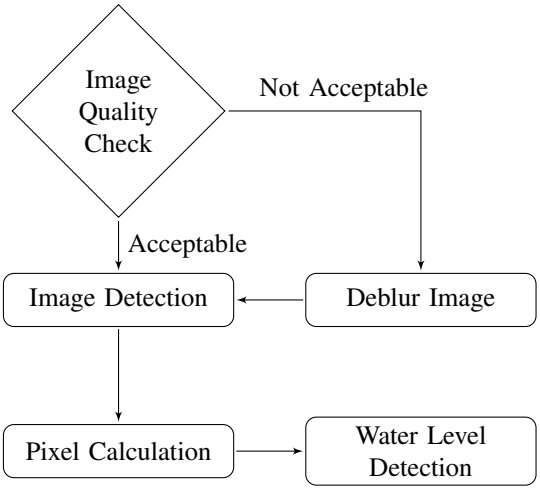

Fig. 1: System overview

background based on a threshold value. To enhance image contrast, histogram equalization (HE) is employed. However, HE methods tend to suffer from over-enhancement and unnecessary noise amplification, leading to a morphology filter. The morphology filter, prevalent in image segmentation, excels in smoothing boundaries in noisy conditions [8]. While the controlled setup of the study in [7] yields highly accurate results, the contrasting reports from [11] demonstrate reduced performance, attributed to image noise and bias towards objects with more significant variances.

In [15], three water level detection methods were evaluated, the difference method, dictionary learning, and a convolutional neural network (CNN) approach. The difference method relies on the stationary nature of the measuring ruler and detects water level changes by comparing consecutive video frames. Dictionary learning segments the image into water and ruler regions to determine the water level. The CNN method, while similar to dictionary learning, utilizes a convolutional neural network for enhanced precision and reliability. However, the study does not elaborate on the performance of these methods under adverse weather conditions. As we will explain further in the paper, the key difference between our proposed approach and this system is that our proposed method addresses water level detection limitations during nighttime and adverse weather conditions. By combining image analysis, deblurring techniques, and the YOLOv5 computer vision technique, we aim to enhance the accuracy and reliability of water level detection in challenging scenarios.

III. Water Level Monitoring in Adverse Weather

This section presents our proposed system for real-time water level detection. Our goal is to detect the water level accurately and continuously in a given environment from collected videos, even in poor weather conditions, including rainy and snowy situations. Fig. 1 depicts the system structure.

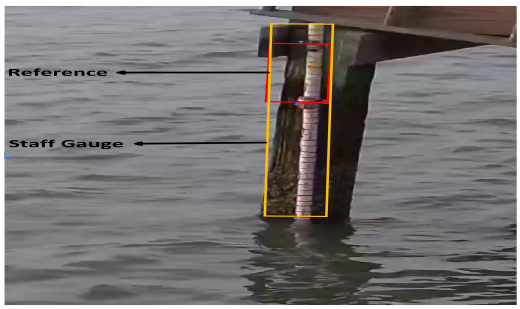

Fig. 2: Measuring staff gauge

A. System Overview

In the proposed system, a standard security camera is utilized to focus on a staff gauge with markers that are evenly spaced. Videos captured by the camera are analyzed to detect the water level against the staff gauge. In our deployment, an in-house-built staff gauge, measuring 220 cm in total length, is employed, with a specific 25-centimeter segment used as a known reference measurement. The gauge setup is shown in Fig. 2. The segment boxed with red lines serves as the reference. During the processing of the gathered images, the image quality of the staff gauge is first assessed. Should the image quality be considered below an acceptable threshold, the Restoration Transformer (Restormer) method, as described in [16], is applied for image deblurring. Next, the YOLOv5 method detects the staff gauge and reference segment. In the final step, pixel calculations are performed to measure the size of the staff gauge above the water, which is then subtracted from the total length of the staff gauge to determine the waterline. This sequential workflow confirms precise measurements, even in challenging image conditions.

B. Image Quality Check

This section explains the method for evaluating the quality of images taken in foggy conditions. This evaluation process can also apply to images captured in various other weather scenarios. For image condition assessment, our approach uses the Peak Signal-to-Noise Ratio (PSNR) [17]. PSNR is a quantitative metric used in image processing to measure the similarity and assess the quality of a reconstructed image compared to its original version. The formulation is presented in Equation (1). A higher PSNR indicates less distortion and higher image quality. PSNR is derived by computing the logarithm of an image's Mean Square Error (MSE). For RGB color images, the calculation of MSE extends to $M \times N$ dimensions, as demonstrated in Equation (2). The PSNR value was generated using the ratio of the log-transformed maximum possible pixel value (MAX) to the MSE. Clear weather images captured during day and night are selected as reference images (I) to check the image quality; differing levels of foggy noise were added to these images, and then their PSNR values were calculated. By comparing the PSNR values of fog-affected images ($\hat{I}$), significant changes are identified that indicate the threshold level for foggy conditions.

$$\text{PSNR} = 10 \cdot \log_{10} \left(\frac{\text{MAX}_I^2}{\text{MSE}} \right) \tag{1}$$

$$MSE = \frac{1}{M \times N} \sum_{x=1}^{M} \sum_{y=1}^{N} [(I_{xyz} - \hat{I}_{xyz})^2] \tag{2}$$

- *Image Processing With Noise-Augmented Techniques:* To start the image augmentation process, a set of 180 images was selected for evaluation, and the PSNR of each image was calculated as the first step. These images were bifurcated into two groups: 90 captured at nighttime and 90 in the daytime. In each set, nine images were associated with a similar noise coefficient ranging from 0.1 to 0.9; the average PSNR number for each coefficient was calculated. The variability in the noise coefficients allowed for the simulation of a range of fog densities, from light mist to heavy fog, creating a comprehensive testing environment. Table I details the average PSNR values calculated for each noise coefficient, linked with the visual representations in Fig. 3 and Fig. 4. These figures show the application of foggy noise coefficients using Albumentations, a method highlighted in [18]. Albumentations, a comprehensive open-source library for image augmentation, utilizes various techniques to simulate diverse weather conditions. This is achieved by applying a range of augmentation coefficients, enabling precise data adjustment and predictions for specific weather scenarios, including rainy, snowy, or foggy conditions.

$$\Delta = \max_{1 \le i < n} |a_{i+1} - a_i| \tag{3}$$

TABLE I: PSNR calculations for different times of day

Daytime		Nighttime	
Picture Name	Average PSNR	Picture Name	Average PSNR
d0.1	35.91	n0.1	48.50
d0.2	35.47	n0.2	48.13
d0.3	34.71	n0.3	48.05
d0.4	31.42	n0.4	47.87
d0.5	29.13	n0.5	29.71
d0.6	28.55	n0.6	29.12
d0.7	28.25	n0.7	28.74
d0.8	28.10	n0.8	28.31
d0.9	27.97	n0.9	28.14

- *Finding the Threshold:* PSNR data for day and night images collected from the previous section were analyzed to find the threshold. A significant change in the PSNR value, according to Equation (3), was evident when examining the data in Table I. This change was particularly pronounced during the nighttime at point n0.5, with a significant drop of 18.2 in the PSNR value compared to the previous point, n0.4. Additionally, in Table I, at point d0.4, there was a 3.3 PSNR drop compared to the preceding point, d0.3. As a result, the threshold point was established as n0.5 for the nighttime case, and for the daytime, the threshold point was determined to be d0.4. These noticeable reductions in the case studies demonstrate the significance of understanding such variations, especially in tasks related to image deblurring, and highlight the importance of setting informed thresholds for decision-making when working with limited data.

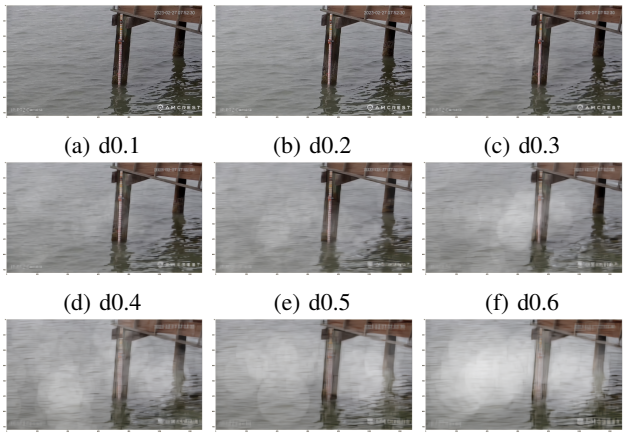

(a) d0.1 (b) d0.2 (c) d0.3 (d) d0.4 (e) d0.5 (f) d0.6 (g) d0.7 (h) d0.8 (i) d0.9

Fig. 3: Day images with different levels of fog noise

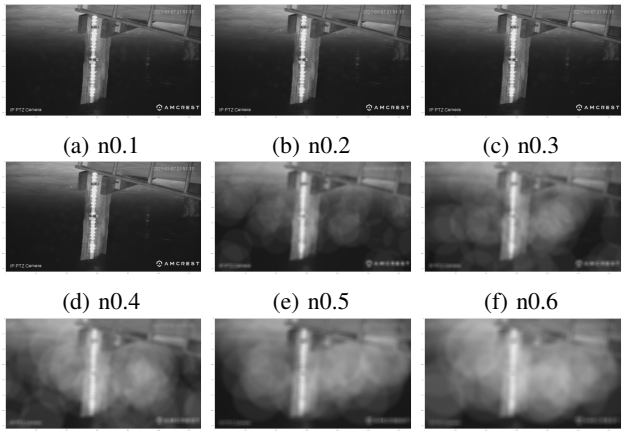

(a) n0.1 (b) n0.2 (c) n0.3 (d) n0.4 (e) n0.5 (f) n0.6 (g) n0.7 (h) n0.8 (i) n0.9

Fig. 4: Night images with different levels of fog noise

C. Deblurring Images

The deblurring process must be implemented if the image quality does not meet the acceptable threshold. We use Restoration Transformer (Restormer) [16], an advanced image-denoising model leveraging deep learning and transformer technology. Restormer introduces a multi-deconv head transposed attention module (MDTA) for enhanced efficiency and a deep convolution gated feed-forward network (GDFN). It processes images through initial low-level feature extraction via a 3×3 convolution, followed by a 4-level encoder-decoder structure for deeper feature development. The model features multiple transformer blocks in its encoder-decoder stages, with MDTA replacing standard

(a) Rain augmentation (b) Snow augmentation

Fig. 5: Images augmentation for different weather conditions

multi-head self-attention for effective high-resolution image processing. MDTA utilizes deep convolution for generating query (q), key (k), and value (v), described in Equations (4) and (5). GDFN within the transformer block ensures selective information passage, filtering features through a gating mechanism.

$$\hat{X} = W_p Attention(\hat{k}, \hat{q}, \hat{v}) + X \tag{4}$$

$$Attention(\hat{q}, \hat{k}, \hat{v}) = \hat{v} \cdot Softmax\left(\hat{k} \cdot \frac{\hat{q}}{\alpha}\right) \tag{5}$$

D. Staff Gauge Detection by YOLOv5

Once the image quality reaches an acceptable level, the dimensions of the staff gauge and the reference part above the waterline are identified and measured in pixels. This study uses the YOLOv5 model [13] is utilized to detect the staff gauge. The YOLOv5 architecture comprises four main components: the input end, the backbone network, the neck feature fusion layer network, and the output end, as shown in Fig. 6. The input end processes the image data, employing Mosaic data enhancement and adaptive scaling. The backbone network, which includes Conv, C3, and SPPF modules, is the primary component for feature extraction. The C3 module within this network integrates residual blocks. The neck network further refines these features, aiming to improve their efficacy for object detection. At the output end, the model uses the CIOU loss function and NMS to precisely identify object locations and categories. YOLOv5's structured design is focused on achieving accurate object detection [19], [20].

Our model was trained using a dataset of 800 annotated images, including two specific labels: one representing the entire staff gauge and another identifying the 25-centimeter measurement indicator, an essential reference. The dataset was divided into training and validating sets in an 8:2 ratio.

E. Pixel Calculation

First, a reference of the staff gauge with a known length (25 cm) in the real world is selected, and this segment is measured in pixels within the image using a YOLOv5 detection coordinate box. The real-world length is then divided by its pixel length to obtain a conversion factor, which allows for translating pixel measurements into actual sizes. To calculate the water level, as shown in Equation (6), the total length of the staff gauge, which is 220 cm, is taken, and the portion above water, measured in pixels, is subtracted from it after converting to centimeters using

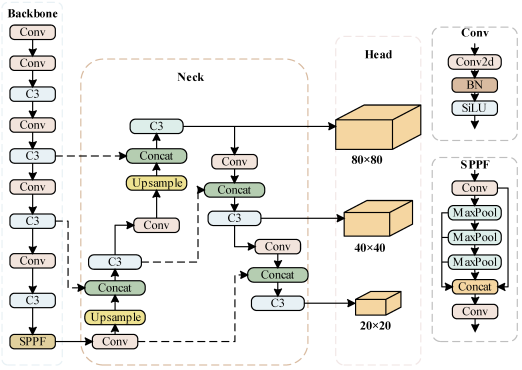

Fig. 6: The YOLOv5 network model diagram (adapted from [20])

the conversion factor. The length of the gauge submerged underwater indicates the waterline depth.

$$Waterlevel(m) = 2.20m - \frac{Staffgauge(pixellength) \times 0.25m}{Reference(pixellength)} \tag{6}$$

IV. Performance Evaluation And Discussion

Based on the image augmentation method, this section assesses the deblurring method's performance. Additionally, the performance of the YOLOv5 detection method with the validation data is analyzed.

A. Methodology and Augmentation Techniques:

Nine groups of images with different noise coefficients for rainy and snowy weather during both daytime and nighttime were generated. The predictions were then meticulously compared to the actual water level value, and the error value was calculated. Afterward, a deblurring method was applied to these images, followed by another comparison with the actual water level value. Finally, average error calculations before and after the deblurring action were evaluated. The weather augmentation method from Albumentations called *RandomRain* and *RandomSnow*, were used for image augmentation techniques. This method generated nine augmented coefficients (with values ranging from 0.1 to 0.9); as shown in Fig. 5, there are augmented image examples.

B. Improvement in Rainy and Snowy Weather:

According to Fig. 7 and Table II, significant improvements are evident in rainy weather conditions. Specifically, during rainy nights, there is a notable improvement of 65.75%, and during rainy days, we observe a substantial improvement of 49.75%. In contrast, there is an improvement of 16.86% for snowy days and 15.60% during snowy nights.

C. Augmented Noise Impact on Water Level Accuracy

The image augmentation technique involves introducing elements like raindrops, snowflakes, and fog into the images. Although this approach helps create a more diverse set of images for analysis, it introduces a significant challenge. The randomness of these elements can interfere with accurately

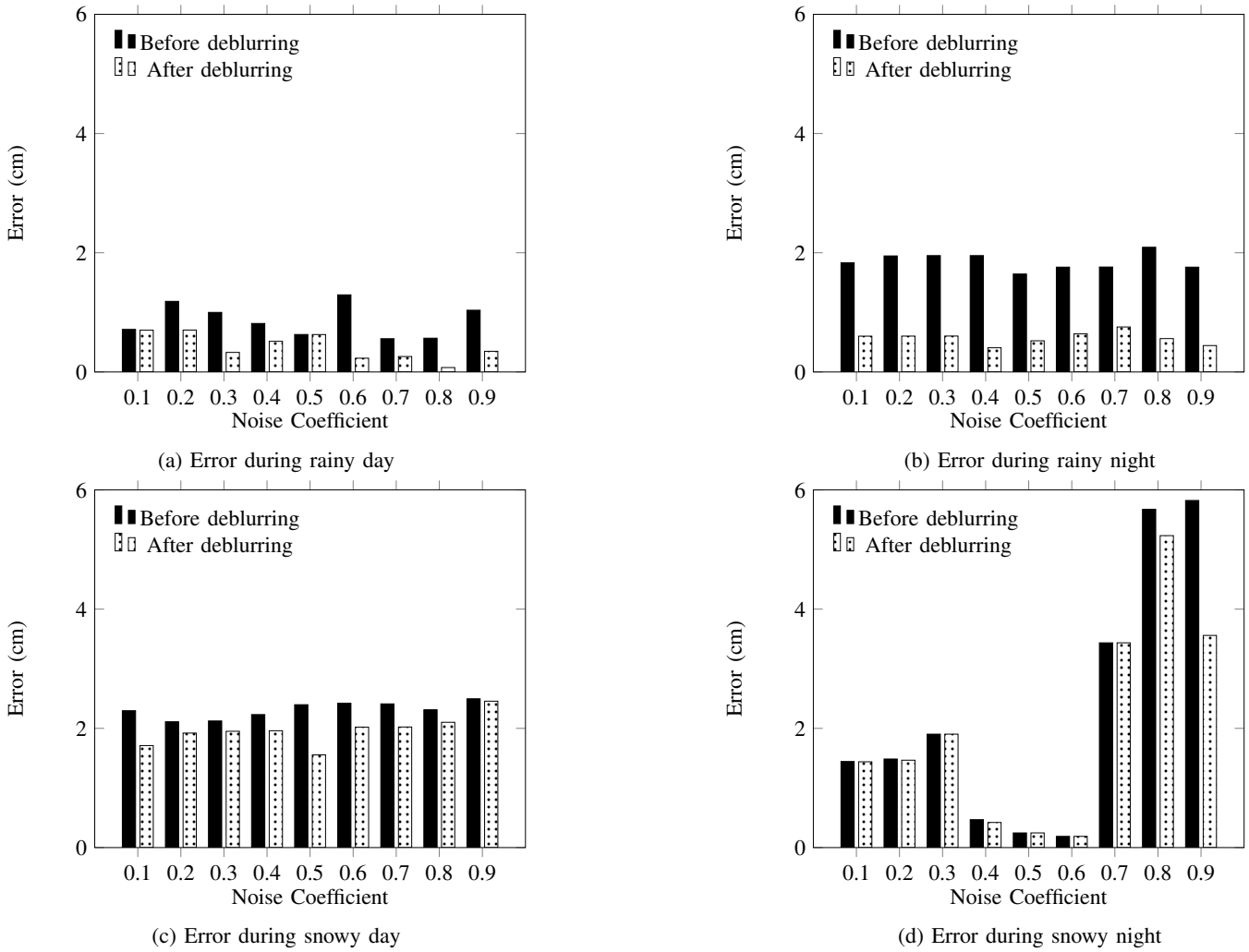

(a) Error during rainy day

(b) Error during rainy night

(c) Error during snowy day

(d) Error during snowy night

Fig. 7: Error in different weather conditions

detecting specific details in the images. This is particularly difficult when determining the pixel size of the staff gauge and its essential reference part.

The increased error rate observed in Fig. 7d (noise coefficients of 0.7, 0.8, and 0.9) is primarily the result of snow noise, which makes the staff gauge reference part hard for YOLOv5 to detect. This interference from snow noise effectively hides the essential features needed for precise water level measurement. This leads to a rise in the error rate as the detection algorithms fail to determine the hidden details against the snowy backdrop accurately.

D. YOLOv5 Detection Evaluation

This experiment used precision and recall as evaluation indices of YOLOv5 model training. Precision (P) is the ratio of the positive samples that are predicted to be correct.

$$Precision = \frac{TP}{TP+FP} \tag{7}$$

TP (True Positive) and FP (False Positive) are correct and incorrect predictions of positives, respectively. FN (False Negative) and TN (True Negative) are incorrect and correct predictions of negatives. Recall (R) is the percentage of positive samples correctly predicted [22].

$$Recall = \frac{TP}{TP+FN} \tag{8}$$

Using Equations (7) and (8), our model shows a precision of 85% and a recall of 100%. Fig. 8 indicates, from testing over 400 epochs, that AP_{50} (average precision at 50% IoU) is 99.2%, and $AP_{50:95}$ (mean precision from 50% to 95% IoU) is 68.7%. Fig. 9 shows our model's effective recognition of the staff gauge and reference in example images, as referenced in [21].

TABLE II: Percentage improvement of an average error

Weather condition	Time	Improvement rate
Rainy	Day	49.75
Rainy	Night	65.75
Snowy	Day	16.86
Snowy	Night	15.60

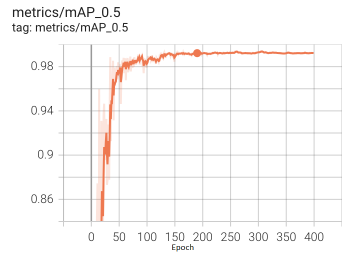

(a) mAP50

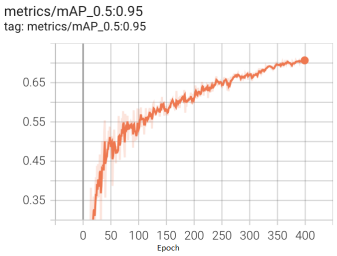

(b) mAP50:95

Fig. 8: mAP50 and mAP50:95

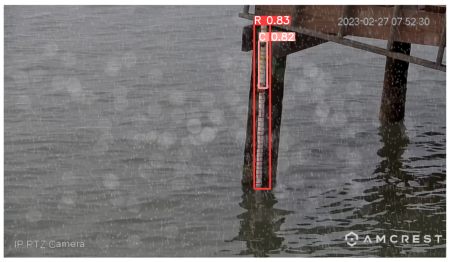

Fig. 9: Image of the YOLOv5 model detection

V. Conclusion and Future Work

This paper presents a novel method for accurate water level detection in adverse weather, utilizing computer vision and image deblurring techniques, including the YOLOv5 framework. This approach overcomes the limitations of traditional measurement methods, proving particularly effective in challenging conditions like nighttime and inclement weather. Our comprehensive system, which involves assessing image quality and applying the Restoration Transformer for deblurring, showed marked improvements in accuracy, especially in rainy conditions.

In future work, the proposed method will be further refined to improve its efficacy during snowy weather conditions, where the observed improvements are currently minimal. The expansion of the dataset, along with the integration of advanced machine-learning techniques, is planned to strengthen the model's robustness and precision. The ultimate goal is to develop a universally adaptable and highly accurate water level detection system that ensures reliability under all weather conditions, contributing significantly to the effectiveness of environmental management and the formulation of disaster prevention strategies.

Acknowledgment

The authors would like to thank the National Science Foundation for supporting this work under Grant No. 2231557. Any opinions, findings, and conclusions or recommendations expressed in this material are those of the author(s) and do not necessarily reflect the views of the National Science Foundation.

References

[1] Y. Zhou, H. Liu, and H. Gao, "In-situ water level measurement using NIRimaging video camera," Flow Meas Instrum, vol. 67, pp. 95–106, 2019.

[2] H.-K. Lee, J. Choo, G. Shin, and S.-M. Kim, "On-site water level measurement method based on wavelength division multiplexing for harsh environments in nuclear power plants," Nucl. Eng. Technol., vol. 52, no. 12, pp. 2847–2851, 2020.

[3] T. L. M. Barreto, J. Almeida, and F. A. M. Cappabianco, "Estimating accurate water levels for rivers and reservoirs by using SAR products: A multitemporal analysis," Pattern Recognit. Lett., vol. 83, pp. 224–233, 2016

[4] M. Moy De Vitry and J. P. Leitao, "˜ The potential of proxy water level measurements for calibrating urban pluvial flood models," Water Res, vol. 175, 2020.

[5] D. Mu et al., "Impact of temporal rainfall patterns on flash floods in Hue City, Vietnam," J. Flood Risk Manag., vol. 14, no. 1, 2021.

[6] K. E. Parnell and H. Kofoed-Hansen, "Wakes from large high-speed ferries in confined coastal waters: Management approaches with examples from New Zealand and Denmark," Coastal Management, vol. 29, pp. 217 –237, 2001.

[7] H. P. Li, W. Wang, F. C. Ma, H. L. Liu, and T. Lv, "The water level automatic measurement technology based on image processing," Appl. Mech. Mater., vol. 303–306, pp. 621–626, 2013.

[8] G. Li, X. Liu, J. Tang, J. Li, Z. Ren, and C. Chen, "De-noising low-frequency magnetotelluric data using mathematical morphology filtering and sparse representation," J. Appl. Geophy., vol. 172, no. 103919, p. 103919, 2020

[9] A. Gao et al., "A newly developed unmanned aerial vehicle (UAV) imagery based technology for field measurement of water level," Water (Basel), vol. 11, no. 1, p. 124, 2019.

[10] Q. Zhang, N. Jindapetch, R. Duangsoithong, and D. Buranapanichkit, "Investigation of image processing based real-time flood monitoring," in 2018 IEEE 5th International Conference on Smart Instrumentation, Measurement and Application (ICSIMA), 2018

[11] Jan, O. R., Jo, H. S., & Jo, R. S. (2021). A critical review on water level measurement techniques for flood mitigation. 2021 IEEE International Conference on Signal and Image Processing Applications (ICSIPA).

[12] J. Redmon, S. Divvala, R. Girshick, and A. Farhadi, "You only look once: Unified, real-time object detection," in 2016 IEEE Conference on Computer Vision and Pattern Recognition (CVPR), 2016.

[13] X. Zhu, S. Lyu, X. Wang, and Q. Zhao, "TPH-YOLOv5: Improved YOLOv5 based on transformer prediction head for object detection on drone-captured scenarios," arXiv [cs.CV], 2021.

[14] Y.-T. Lin, Y.-C. Lin, and J.-Y. Han, "Automatic water-level detection using single-camera images with varied poses," Measurement (Lond.), vol. 127, pp. 167–174, 2018.

[15] J. Pan, Y. Yin, J. Xiong, W. Luo, G. Gui, and H. Sari, "Deep learning-based unmanned surveillance systems for observing water levels," IEEE Access, vol. 6, pp. 73561–73571, 2018

[16] S. W. Zamir, A. Arora, S. Khan, M. Hayat, F. S. Khan, and M.-H. Yang, "Restormer: Efficient transformer for high-resolution image restoration," in 2022 IEEE/CVF Conference on Computer Vision and Pattern Recognition (CVPR), 2022

[17] F. A. Fardo, V. H. Conforto, F. C. de Oliveira, and P. S. Rodrigues, "A formal evaluation of PSNR as quality measurement parameter for image segmentation algorithms," arXiv [cs.CV], 2016.

[18] B. Alexander, E. K. Vladimir, and I. I. Alexandr, Albumentations: fast and fexible image augmentations.

[19] Z. Xu, G. Yang, and Y. Zhang, "Road target detection algorithm based on improved YOLOv5," in 2023 IEEE 7th Information Technology and Mechatronics Engineering Conference (ITOEC), 2023.

[20] Z. Ren, H. Zhang, and Z. Li, "Improved YOLOv5 network for real-time object detection in vehicle-mounted camera capture scenarios," Sensors (Basel), vol. 23, no. 10, 2023.

[21] X. Liu, G. Tang, and W. Zou, "Improvement of detection accuracy of aircraft in remote sensing images based on YOLOV5 model," in 2021 IEEE International Geoscience and Remote Sensing Symposium IGARSS, 2021.

[22] Z. Zhang, X. Lin, K. Yang, and H. Wang, "An improved merge-YOLOv5 algorithm for infant monitoring," in 2022 5th International Conference on Pattern Recognition and Artificial Intelligence (PRAI), 2022.